blood®
Regular Article

LYMPHOID NEOPLASIA

Integrative genomic analysis identifies key pathogenic mechanisms in primary mediastinal large B-cell lymphoma

Anja Mottok,[1-3,*] Stacy S. Hung,[1,*] Elizabeth A. Chavez,[1] Bruce Woolcock,[1] Adèle Telenius,[1] Lauren C. Chong,[1] Barbara Meissner,[1] Hisae Nakamura,[1] Christopher Rushton,[4] Elena Viganò,[1] Clementine Sarkozy,[1] Randy D. Gascoyne,[1,2] Joseph M. Connors,[1] Susana Ben-Neriah,[1] Andrew Mungall,[5] Marco A. Marra,[5] Reiner Siebert,[3] David W. Scott,[1] Kerry J. Savage,[1] and Christian Steidl[1,2]

[1]British Columbia Cancer, Centre for Lymphoid Cancer, Vancouver, BC, Canada; [2]Department of Pathology and Laboratory Medicine, University of British Columbia, Vancouver, BC, Canada; [3]Institute of Human Genetics, Ulm University and Ulm University Medical Center, Ulm, Germany; [4]Department of Molecular Biology and Biochemistry, Simon Fraser University, Burnaby, BC, Canada; and [5]British Columbia Cancer, Canada's Michael Smith Genome Sciences Centre, Vancouver, BC, Canada

KEY POINTS

- **Whole-exome sequencing and gene expression profiling reveal genetic driver alterations and elucidate pathway dependencies in PMBL.**
- **Comparative analysis points to relevant differences to diffuse large B-cell lymphoma and highlights the pathological and molecular relatedness to cHL.**

Primary mediastinal large B-cell lymphoma (PMBL) represents a clinically and pathologically distinct subtype of large B-cell lymphomas. Furthermore, molecular studies, including global gene expression profiling, have provided evidence that PMBL is more closely related to classical Hodgkin lymphoma (cHL). Although targeted sequencing studies have revealed a number of mutations involved in PMBL pathogenesis, a comprehensive description of disease-associated genetic alterations and perturbed pathways is still lacking. Here, we performed whole-exome sequencing of 95 PMBL tumors to inform on oncogenic driver genes and recurrent copy number alterations. The integration of somatic gene mutations with gene expression signatures provides further insights into genotype–phenotype interrelation in PMBL. We identified highly recurrent oncogenic mutations in the Janus kinase-signal transducer and activator of transcription and nuclear factor κB pathways, and provide additional evidence of the importance of immune evasion in PMBL (*CIITA, CD58, B2M, CD274,* and *PDCD1LG2*). Our analyses highlight the interferon response factor (IRF) pathway as a putative novel hallmark with frequent alterations in multiple pathway members (*IRF2BP2, IRF4,* and *IRF8*). In addition, our integrative analysis illustrates the importance of *JAK1, RELB,* and *EP300* mutations driving oncogenic signaling. The identified driver genes were significantly more frequently mutated in PMBL compared with diffuse large B-cell lymphoma, whereas only a limited number of genes were significantly different between PMBL and cHL, emphasizing the close relation between these entities. Our study, performed on a large cohort of PMBL, highlights the importance of distinctive genetic alterations for disease taxonomy with relevance for diagnostic evaluation and therapeutic decision-making. (*Blood*. 2019;134(10):802-813)

Introduction

Over the past decade, a number of studies have unraveled the molecular and genetic heterogeneity of lymphoid malignancies, leading to the recognition of new entities and refinement of the existing taxonomy in the form of the World Health Organization (WHO) classification.[1] In the broader context of the development of alternative treatment options, including the testing of novel drugs and/or combinations, coupled with refining a more personalized medicine approach, evidence is accumulating that disease classification plays an important role for patient risk stratification and therapeutic decision-making.

Large B-cell lymphomas account for >40% of B-cell non-Hodgkin lymphomas (NHL), representing the most common subtype worldwide.[1] Diffuse large B-cell lymphoma (DLBCL), an aggressive cancer requiring immediate treatment, is the most common B-cell NHL and exemplifies the relevance of molecular subclassification and comprehensive genomic characterization for understanding fundamental disease biology and improving patient care.[2-7] In contrast, primary mediastinal large B-cell lymphoma (PMBL) represents a relatively rare subtype, accounting for only 2% to 3% of B-cell NHL and 10% of large B-cell lymphomas. Its characteristic presentation features a predominant anterior mediastinal mass in young adults, with a higher prevalence in female subjects.[1] Molecular studies in the past have provided evidence that PMBL truly typifies a distinct large B-cell lymphoma entity. In particular, gene expression profile analyses have shown that PMBL is more closely related to classical Hodgkin lymphoma (cHL)[8,9] despite the fact that its morphological features are mostly reminiscent of DLBCL in

terms of cell size, phenotype, and infiltration pattern.[1,10] Although PMBL has been recognized as a distinct lymphoma entity in the WHO classification since 2008,[1] diagnosis in most cases is still based on a clinico-pathological consensus that is not always well instituted and has a subjective component. This approach is in part due to the fact that gene expression profiling has not yet fully entered routine clinical practice, a problem that may be overcome by broader implementation of technologies using archival tissue specimens.[11-13] Moreover, the correct identification of PMBL can be difficult because PMBL(-like) cases have been observed at non-mediastinal sites,[14] and so-called mediastinal gray-zone lymphomas present another challenge in the spectrum of differential diagnoses.[15-17]

Since the first description of PMBL, a number of recurrent somatic gene mutations, copy number (CN) alterations, and frequently occurring structural genomic alterations have been identified. Constitutive activation of oncogenic signaling on the basis of mutations in the nuclear factor κB (NF-κB) and Janus kinase-signal transducer and activator of transcription (JAK-STAT) pathways is recognized as a hallmark of this disease.[18,19] Moreover, key discoveries connecting genetic alterations with immune escape properties of lymphoma cells have highlighted the role of the tumor microenvironment in cancerogenesis[20] and have spurred the implementation of immunotherapies, such as immune checkpoint blockade.[21,22] Similar to cHL, PMBL harbors genomic aberrations leading to an immune privilege phenotype; namely, recurrent alterations targeting the class II transactivator *CIITA*,[23,24] the master transcriptional regulator of major histocompatibility complex (MHC) class II, and numerical and structural genomic changes of the 9p24.1 locus[25-28] (including the 2 programmed death 1-receptor ligands *CD274* and *PDCD1LG2*) have been characterized as important aspects in PMBL pathogenesis.

Although targeted sequencing studies have revealed a number of key genetic lesions involved in PMBL lymphomagenesis, a comprehensive description of genetic alterations in a sizeable cohort of patients is still lacking. In the current study, we performed whole-exome sequencing of 95 PMBL tumors, most of which have also been molecularly defined by using the recently described Lymph3Cx assay.[13] By systematically integrating mutational and gene expression profiles, we inform on oncogenic driver genes and recurrent CN alterations and describe new potential pathway dependencies. In addition, the intersection of driver genes found in related entities further substantiates the close relationship between PMBL and cHL.

Methods

Patient cohort and clinico-pathological characteristics

Patients were selected from the clinical database of the British Columbia Cancer, Centre for Lymphoid Cancer, based on a recorded (clinico-)pathological diagnosis of PMBL and clinical follow-up data. Specimens were retrieved from tissue archives of the Centre for Lymphoid Cancer or referring hospitals. In total, 118 biopsy specimens with the histopathological diagnosis of PMBL were identified that had all been previously reviewed by an expert panel of hematopathologists of the Lymphoma/Leukemia Molecular Profiling Project[13] using criteria published in the 2008 WHO classification.[1] Ninety-five of these cases were selected for this study based on availability of tissue, fresh-frozen cell suspensions, or tumor DNA. For 91 of 95 specimens, tumor content information was available and estimated to exceed 30% based on hematoxylin and eosin staining in 86 cases; 5 cases were macrodissected to enrich for tumor content or to exclude necrotic tumor areas. Tumor content information was not retrievable for 4 cases. Constitutional DNA from peripheral blood was available for 21 patients (in 12 cases, formalin-fixed, paraffin-embedded tissue-derived corresponding tumor DNA and in 9 cases, tumor DNA derived from cell suspensions was sequenced). The clinical characteristics are summarized in Table 1 and detailed information on study design, molecular classification, and available data per patient is given in supplemental Figure 1 (available on the *Blood* Web site).

Table 1. Clinical characteristics of the PMBL cohort (N = 95)

Clinical characteristic	n (%)
Sex	
Female	54 (56.8)
Male	41 (43.2)
Age, median (range), y	34 (13-79)
Stage	
I/II	70 (73.7)
III/IV	24 (25.3)
NA	1 (1)
Biopsy site	
Mediastinum	59 (62.1)
Local or cervical lymph nodes, lung	29 (30.5)
Inguinal lymph node, paraspinal L1	2 (2.1)
NA	5 (5.3)
IPI group	
Low	41 (43.1)
Intermediate	39 (41.1)
High	11 (11.6)
NA	4 (4.2)
Bulky disease (>10 cm)	
Yes	70 (73.7)
No	24 (25.3)
NA	1 (1)
Rituximab-containing therapy	
Yes	59 (62.1)
No	33 (34.7)
NA	3 (3.2)

IPI, International prognostic index; NA, not available.

This study was approved by the Research Ethics Board of the University of British Columbia and British Columbia Cancer (REB file H14-02304). Patients either provided written informed consent or a waiver of consent was in place for cases collected previously.

Whole-exome sequencing

DNA extraction was performed as previously described.[24] DNA was derived from fresh-frozen cell suspensions in 32 cases and

from formalin-fixed, paraffin-embedded tissue in 63 cases. Whole-exome sequencing was performed by using a targeted capture approach with the SureSelect Human All Exon V6+UTR bait (Agilent Technologies) followed by massively parallel sequencing of enriched fragments on the HiSeq 2500 platform (Illumina). Five libraries were pooled per lane, and a 125 bp paired-end mode was used. Tumor and normal DNA samples were sequenced to an average of 115X (standard deviation: 24X). All reads were aligned to the human reference genome (hg19) by using bwa-mem version 0.7.5a[29] with optical and polymerase chain reaction duplicates removed by using the Picard tool (http://broadinstitute.github.io/picard/).

Identification of somatic single nucleotide variations and indels

For cases with paired normal DNA, somatic single nucleotide variation (SNV)/indel variants were identified by using the intersection of calls predicted by VarScan (version 2.3.6),[30] Strelka (version 1.0.13),[31] and MuTect (version 1.1.4),[32] with a minimum variant allele frequency of 1% and 10 variant reads. For unpaired tumor specimens (n = 74), somatic SNV/indel variants were identified by using VarScan and required to have a minimum variant allele frequency of 5% and 10 variant reads. Putative germline variants were removed by using virtual normal correction.[33] In addition, any variant associated with an identifier in dbSNP version 137[34] was discarded. All variants were annotated by using SnpEff (version 4.2)[35] and filtered for effects predicted to have a moderate or high impact at the protein level (ie, nonsynonymous, stop gained, splice site acceptor mutations).

MutSigCV analysis

The statistical significance of mutation frequency in each gene was determined by using the MutSigCV algorithm (http://software.broadinstitute.org/cancer/software/genepattern/modules/docs/MutSigCV).[36] To accurately estimate the background mutation rate, synonymous mutations in addition to the full set of (nonsynonymous) somatic SNVs and indels identified through the paired SNV calling pipeline were analyzed. Because the default coverage file provided by MutSigCV may not properly represent the target space used by our capture bait, CovGen (https://github.com/tgen/CovGen) was used to provide an accurate estimate of coverage in the cohort. We used the default covariate table provided by MutSigCV, which contains the following variables for each gene: (1) global expression; (2) DNA replication time; and (3) HiC statistic. Due to our limited cohort size, $P < .05$ was used to obtain a list of candidate driver genes. From this list, only genes present in RefSeq were included for downstream analyses. Three genes (C21orf91, C11orf94, and C6orf226) had open reading frames with uncharacterized proteins and were therefore removed.

CN analysis

CN alterations for all tumor specimens were called by using the CNVkit[37] with default thresholds (if $\log2 \leq -4.3$, CN = 0; if $\log2 \leq -1$, CN = 1; if $\log2 \leq 0$, CN = 2; if $\log2 \leq 0.6$, CN = 3) assuming a ploidy of 2 (further details are given in the supplemental Methods).

To identify relevant regions of CN alterations, the GISTIC (Genomic Identification of Significant Targets in Cancer) method described by Beroukhim et al[38] was applied to the curated segmentation results (further details are given in the supplemental Methods).

Gene expression analysis and *xseq*

Gene expression data (DASL platform, HumanHT-12 v4.0 Expression BeadChip; Illumina) was available for 70 of 95 cases. RNA was extracted by using either the RNeasy Mini Kit or the AllPrep FFPE kit (Qiagen) and measured by using a NanoDrop spectrophotometer (Thermo Fisher Scientific). Nucleic acids were diluted to a final concentration of 100 ng/μl, and array hybridization was performed at The Hospital for Sick Children (Toronto, ON, Canada) using the HumanHT-12 v4.0 Expression BeadChip. The limma and beadarray R packages were used to analyze probe-level expression data. A normal-exponential convolution model was applied for background correction and normalization of the data, followed by log2 transformation and quality assessment. Probes below the detection score (ie, considered to be not expressed) in at least 3 arrays were removed (27 446 probes remained). One case of the sequencing cohort was identified as an outlier by both multidimensional scaling and principal component analysis, and was therefore removed. After exclusion of case PA012, a total of 68 cases were available for integrative analyses. Annotation of probes with quality and gene symbol information was performed by using the illuminaHumanv4.db probe annotation database (Illumina). Probes annotated as having "bad" quality or that had no gene match were removed. A total of 24 501 probes representing 17 027 genes remained, with 4659 of those being represented by >1 probe (ie, ambiguous transcript).

For both the *cis*- and *trans*-analysis (ie, mutations that affect gene expression of the same gene or a set of other genes, respectively), the *xseq* method was applied.[39] Further details are given in the supplemental Methods.

Statistical analyses

Fisher's exact test and, when appropriate, the χ^2 test were used to assess whether differences in categorical variables (eg, frequency of mutated cases in different disease groups) were significant between groups. Statistical significance was defined as $P < .05$. All analyses were performed in R, the statistical programming language (R Core Team, 2017).

Results

The mutational landscape of PMBL identified by whole-exome sequencing

To characterize the full spectrum of coding sequence mutations in a large cohort of PMBL cases, we performed whole-exome sequencing in 95 patient-derived tumor specimens. Matched constitutional DNA was available for 21 cases. The clinical characteristics of these patients are described in Table 1. One tumor-normal pair was removed due to high similarity with the normal (likely due to insufficient tumor content in the frozen cell suspension), resulting in 20 paired cases that were used for downstream analysis.

By applying a robust bioinformatics pipeline integrating 3 variant callers (see "Methods" for details), 7200 somatic mutations were identified across the cohort of paired samples. Of those, 3120 were nonsynonymous (missense and nonsense), 1212 were

synonymous, 2391 were nonexonic (3′- or 5′-untranslated region [UTR]), 73 were splice site alterations, and 404 were small indels (supplemental Figure 2A). After removal of silent and UTR variants, the median number of putatively protein-altering mutations per case was 155 (range, 44-741) in paired specimens (supplemental Figure 2B). A list of genes recurrently affected by UTR mutations is provided in supplemental Table 1.

Mutations in the unpaired specimens (n = 74) were filtered to exclude silent and UTR mutations, resulting in a median of 683 (range, 411-1227) protein-altering variants (SNVs and small indels) per case. The median number of variants in the unpaired specimens was significantly higher compared with the paired samples, attributable to the presence of private single nucleotide polymorphisms and platform noise that was not immediately filterable. In both paired and unpaired cases, *SOCS1* (suppressor of cytokine signaling 1) was the most commonly mutated gene (64%). A complete list of 94 genes, which were mutated in at least 10% of all cases and 10% of paired cases (to reduce the number of likely artifacts), is provided in supplemental Table 2. We found frequently altered and previously identified[18,40-43] genes involved in JAK-STAT signaling (*STAT6* [signal transducer and activator of transcription 6], *PTPN1* [protein tyrosine phosphatase nonreceptor type 1], *IL4R* [interleukin-4 receptor], *JAK1, CISH* [cytokine-inducible SH2-containing]), NF-κB signaling (*TNFAIP3* [tumor necrosis factor, α-induced protein 3], *NFKBIE* [NFKB inhibitor ε], *NFKB2* [NFKB subunit 2], and *IKBKB* [inhibitor of NFKB kinase subunit β]), and immune escape (*CIITA, B2M* [β_2-microglobulin], and *CD58* [cluster of differentiation 58]) (supplemental Figure 3A). Comparison of the median variant allele frequencies of these genes provides evidence that mutations in genes such as *IL4R, FAT1* (FAT atypical cadherin 1), and *EP300* (E1A binding protein P300) might occur early in PMBL pathogenesis, whereas those in *CIITA, ACTB* (actin β), and *BTG1* (BTG antiproliferation factor 1) seem to be late events (supplemental Figure 3B). Interestingly, multiple genes involved in interferon response (IRF) were mutated in ∼10% of the tumors each. In particular, we found mutations in *IRF1*, *IRF4, IRF8,* and *IRF2BP2* with identification of a hotspot mutation *IRF4*:c.295T>C, p.(Cys99Arg) in >50% of *IRF4*-mutated cases (supplemental Figure 4A). Overall, genetic alterations in these interferon response genes and related downstream targets were found in 52% of our cohort. Further analysis on a case-by-case level revealed a pattern reminiscent of mutual exclusivity, pointing toward a convergent role in PMBL pathogenesis (supplemental Figure 4B).

Oncogenic driver genes in PMBL

The tumor-normal pairs (n = 20) were used as a primary discovery set to identify potential genetic "drivers" (ie, gene mutations with high impact on disease pathogenesis) in PMBL, with the remaining cases serving as an internal validation set to ensure the reproducibility of findings, as well as an extension cohort to further characterize mutation frequencies and clinical correlates in the full set of 94 tumors. Application of MutSigCV[36] to the distribution of somatic alterations in the discovery cohort revealed 50 putative driver genes that were recurrently and significantly mutated in PMBL (significance cutoff, $P < .05$) (supplemental Table 3). This gene set prominently included members of the JAK-STAT and NF-κB–signaling pathways (*SOCS1*, *STAT6, PTPN1*, *IL4R, CISH, TNFAIP3, NFKBIE,* and *TRAF3* [TNF receptor associated factor 3]), genes known to be involved in immune escape (*CIITA, CD58,* and *IL13RA*), and interestingly several interferons and interferon-regulatory factors (*IRF2BP2, IRF8,* and *IRF4).* In line with these findings, gene ontology enrichment analysis depicted pathways related to B-cell activation, antigen processing and presentation, complement activation, IFN signaling, and Fc-γ receptor signaling (supplemental Figure 5A).

We next identified genetic alterations corresponding to these 50 candidate driver genes in all PMBL cases (n = 94); mutational frequencies, mutation types, and clinical/molecular features are displayed in Figure 1. Similarly, as described earlier, comparison of the median variant allele frequencies of these 50 candidate drivers suggests that mutations in genes such as *IL4R, DDX3X* (DEAD-box helicase 3), *CD58*, and *NFKBIE* occur early in PMBL pathogenesis, whereas *CIITA, JUNB* (JunB proto-oncogene, AP-1 transcription factor subunit), and *KLF9* (Krüppel-like factor 9) are late events (supplemental Figure 5B). As an alternative approach, we used the OncodriveCLUST tool[44] to identify potential driver genes in this dataset. A total of 29 genes were identified with only 5 genes having a false discovery rate (FDR) <0.1 (*IRF4, EZH2* [enhancer of zeste homolog 2], *STAT6, HIST1H3D,* and *ACTB*) (supplemental Figure 6). Of note, these genes were also identified by MutSigCV.

Interestingly, when analyzing genetic alterations (including UTR and silent mutations) with regard to mutational signatures as defined by Alexandrov et al,[45] we found an association of mutation patterns with aging, defective DNA mismatch repair, and AID/APOBEC activity (supplemental Figure 5C-E). Although the correlation with an "aging" signature seems counterintuitive in a patient population with a median age at diagnosis of 34 years, similar findings were reported in other cancers, including pediatric tumors.[46] These findings might be reflective of the high proliferation and cell division count that is not necessarily linkable to the "chronological age" of the patient.

To investigate if genetic alterations in the identified candidate driver genes show patterns of co-occurrence or mutual exclusivity, we performed pairwise testing (Fisher's exact test) followed by multiple test correction (Benjamini-Hochberg method). A number of significant correlations were identified between certain genetic lesions (Figure 2A), including 3 mutually exclusive pairs (*SOCS1* and *CXCR5* [CXC motif chemokine receptor 5]; *GNA13* [guanine nucleotide-binding protein subunit α-13] and *IL4R*; *STAT6* and *CISH*) (corrected $P < .05$) (Figure 2B). Examples for significantly co-occurring mutations (*ACTB* and *IRF2BP2*; *ZFP36L1* and *CISH*) are depicted in supplemental Figure 7 ($P < .05$).

Recurrent CN alterations in PMBL cooperate with mutations in pathways related to immune evasion and oncogenic signaling

In addition to SNVs and indels, we characterized CN alterations across all 94 exomes using CNVkit,[37] a tool that utilizes both on- and off-target coverage to infer CN evenly across the genome (supplemental Figure 8). GISTIC[38] was then applied to identify regions of statistically significant gains or losses (Figure 3A). Consistent with earlier literature, the most significant regions of CN gain were located on 9p (*CD274* and *PDCD1LG2*; 72% of tumors showing CN gain) (Figure 3B), 2p (*REL*; 36%), 6p (47%), and 11q (40%). Although CN losses are poorly characterized in

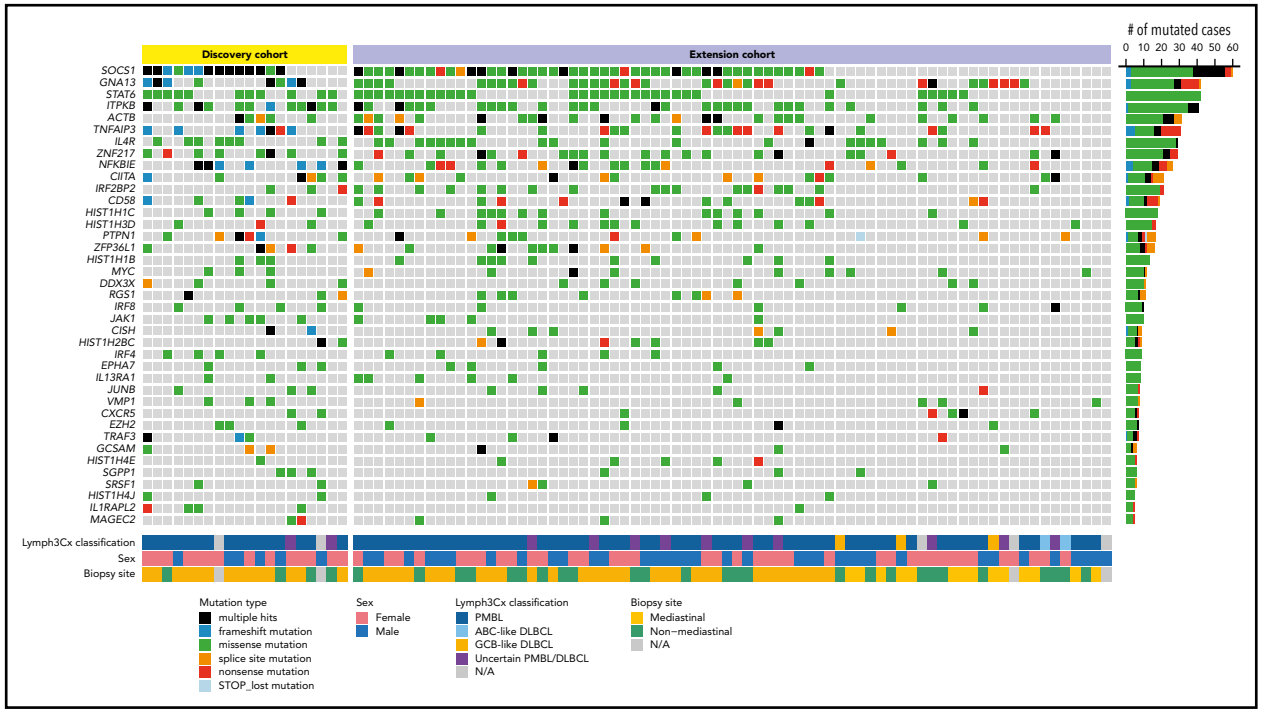

Figure 1. Putative driver genes in PMBL pathogenesis as identified by using MutSigCV. Each column in this plot represents an individual case (with mutation[s] in the displayed genes) of the final PMBL sequencing cohort (n = 94), separated into the discovery and extension cohort. Recurrently and significantly mutated genes (as identified by using the MutSigCV algorithm,[36] $P < .05$) constitute individual rows and are sorted according to their mutational frequencies (in the form of absolute numbers of mutated cases as provided on the far right; note that for visualization purposes, of the fifty identified genes only genes mutated in ≥5% of the entire cohort are displayed). Tracks at the bottom of the plot provide information on molecular classification (using the Lymph3Cx assay[13]), sex, and biopsy site. Mutation types are color-coded as indicated in the key. ABC, activated B-cell; GCB, germinal center B-cell; N/A, not available.

PMBL, we found that the most frequent regions of loss identified in our study (chromosomes 10q, 8p, 1p, and 7p; all >30%) were consistent with those identified in the study by Wessendorf et al,[47] which is the largest PMBL genome-wide CN study performed to date. Details on chromosomal location, including genes and statistics of significant regions of deletions and gains/amplifications, are provided in supplemental Table 4, and the distribution of these CN alterations across the PMBL cohort is shown in supplemental Figure 9B.

Contrasting mutational landscapes to related pathological entities

To define more clearly the commonalities and differences between PMBL and related pathological entities (ie, DLBCL and cHL), we compared the mutational driver genes in PMBL as described earlier vs 2 large cohorts of DLBCL[4,48] (n = 304 and n = 1001, respectively) and the largest cHL exome cohort studied to date (n = 34).[49] Interestingly, PMBL driver genes mutated in ≥3 tumors exhibited dramatically lower mutational frequencies in the cohort of patients with DLBCL reported by Reddy et al[48] (Figure 4A). When we compared mutational frequencies in a panel of genes, representing the driver genes in DLBCL as reported by Chapuy et al[4] (supplemental Figure 10), we could clearly show that, with the exception of *EZH2*, the frequencies of mutations in all these genes were statistically significantly different ($P < .05$) between PMBL and DLBCL (Figure 4B). In contrast, frequencies of recurrently mutated genes in cHL trended similarly to corresponding frequencies in the PMBL cohort, with only 3 genes (*IGLL5*, *ITPKB*, and *NUP214*) displaying a statistically significant difference ($P < .05$) (Figure 4C).

To better understand potential contrasting genomic underpinnings in tumors reflecting the molecular spectrum of PMBL and DLBCL, we next compared mutational profiles in our PMBL cohort based on molecular classification according to the Lymph3Cx assay.[13] Interestingly, by contrasting mutational frequencies in bona fide PMBL (as assigned by the molecular classifier, n = 73) vs the cohort comprising molecularly defined DLBCL (n = 5) and tumors placed in the "uncertain" category (n = 12), we identified *IL4R* as being significantly enriched in the molecular PMBL group (with no mutations found in the other groups); *TNFRSF14* was only found to be mutated in molecularly defined non-PMBL tumors (supplemental Figure 11A-C). Of note, when we analyzed the tumors with available gene expression data (DASL platform) based on the genes included in the recently published molecular classifier,[13] we obtained a similar pattern, with the molecular DLBCLs forming a separate cluster, pointing to the stability of the gene expression–based model (supplemental Figure 12).

Integrative analysis

We next performed an integrated mutation–gene expression analysis using *xseq*[39] to ascertain the impact of recurrent mutations on transcriptional profiles. Specifically, the approach aims at assessing the likely association of present mutations with observed deviations from neutral expression measurements in the same tumor. Examining the "*cis*-effect" of loss-of-function mutations (frameshift, nonsense, and splice site mutations) on gene expression, *NBPF1* (neuroblastoma breakpoint family, member 1), mutated in 30 tumors, was identified with high certainty [*P*(D) = .9942] to have an influence on gene expression

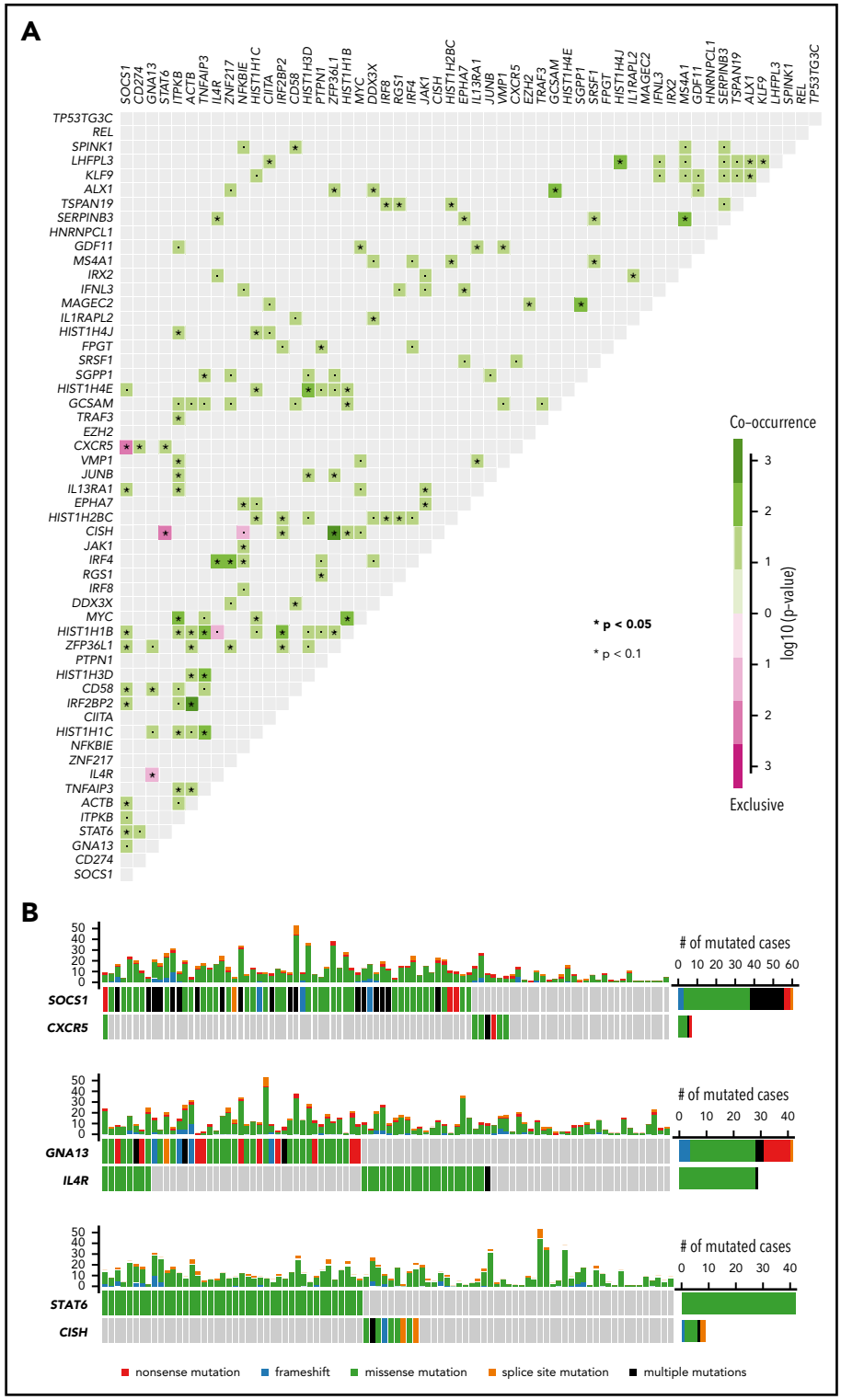

Figure 2. Mutational patterns and correlation of genetic alterations in PMBL. (A) Statistically significant mutual exclusivity or co-occurrence among the identified PMBL driver genes using pairwise Fisher's exact test (multiple testing correction was performed according to the Benjamini-Hochberg method). (B) Highly significant examples of mutual exclusivity (*SOCS1* and *CXCR5*, *GNA13* and *IL4R*, *STAT6* and *CISH*) are shown as pairwise comparisons. Each column represents a case, and mutated cases are highlighted in colors indicating specific mutation types as specified in the key. Absolute numbers of mutated cases are provided on the right, and the frequency plot on top of each subpanel provides the number of mutations in driver genes per case.

in its mutated form (Figure 5A), with 3 other genes (*FRG1*, *STAT6*, and *ZNF681*) having considerable "*cis*-effects" on gene expression but with probability levels below the recommended cutoff [*P*(D) < .8]. In contrast, a number of mutated genes exhibited "*trans*-effects" on gene expression with high-confidence probabilities (*P*(D) > 0.8). The distribution of mutations in those genes across the sequencing cohort with available gene expression data (n = 68) revealed alterations in at least 1 of these 15 genes on an individual case level (Figure 5B). Most prominently, we identified among the significantly *trans*-influencing genes, *JAK1* and *RELB*, members of the JAK-STAT and NF-κB pathways, respectively. Both pathways are known activated oncogenic pathways in PMBL, although the importance of *JAK1* and *RELB* mutations as drivers of differential expression programs has not been described before. The respective gene association networks with functionally enriched

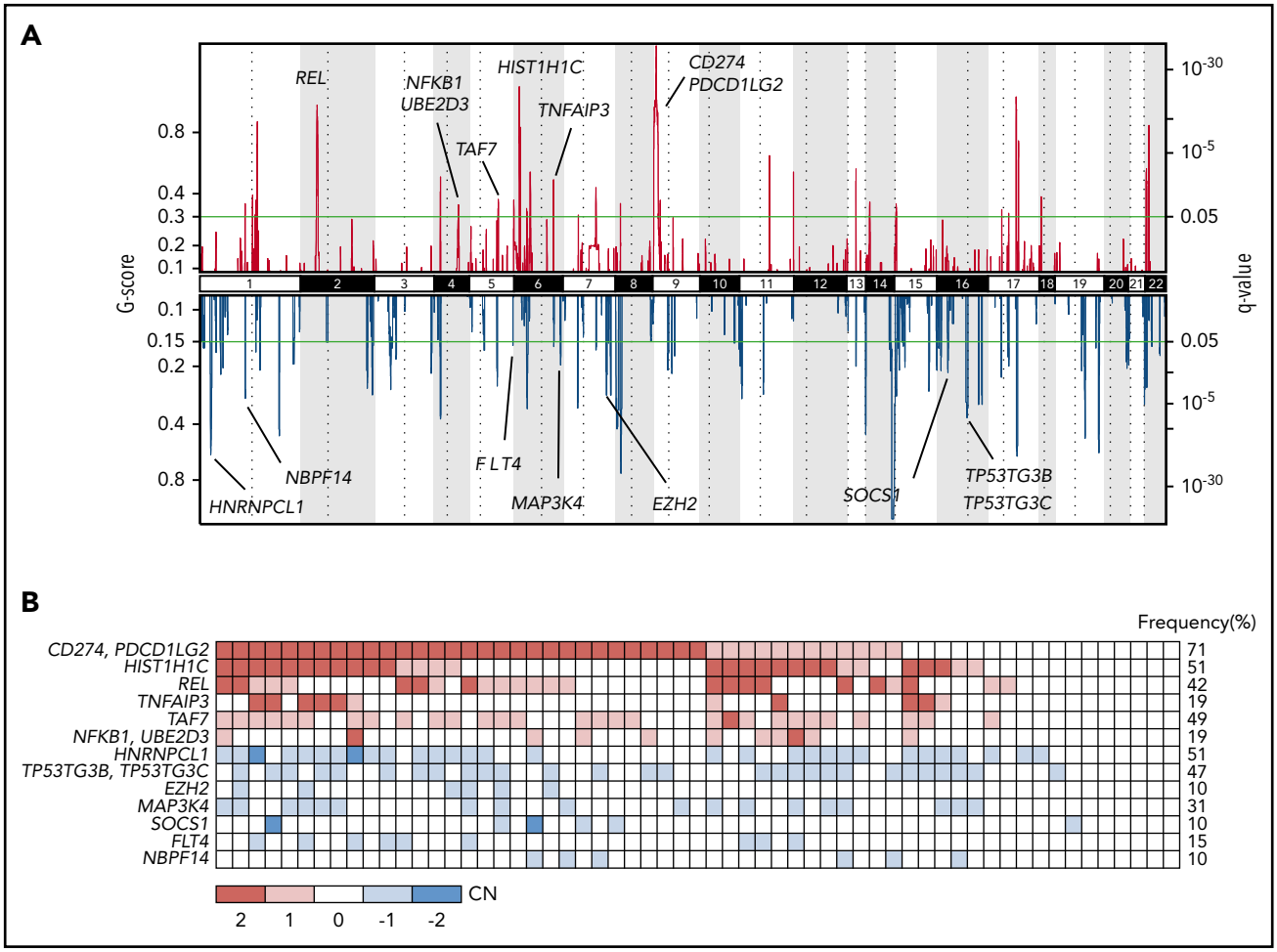

Figure 3. Recurrent CN alterations in PMBL. (A) Significant CN gains (red) and losses (blue) as inferred from whole-exome sequencing data using GISTIC 2.0. Potential candidate genes are highlighted next to their respective genomic locus. (B) Frequency plot of genes displaying significant CN alterations across the cohort. Red indicates CN gain, and blue indicates CN loss, where values are derived from GISTIC and indicate copy-number level per gene: −2 = homozygous deletion; −1 = heterozygous deletion; 0 = CN unchanged; 1 = low-level gain; 2 = high-level gain/amplification. Genes were sorted according to gain/deletion and then per *q* value as calculated by using GISTIC.

pathway members are displayed in Figure 5C and 5D, respectively. *EP300,* a histone acetyltransferase that functions as a coactivator of many transcription factors to regulate gene transcription, plays an important role in hematopoiesis and has been found mutated in other hematological malignancies.[50,51] Figure 5E displays the gene association network and indicates quantitative changes in gene expression of functionally enriched pathway members.

Discussion

The current article reports on whole-exome sequencing data obtained in a cohort of 94 PMBL tumors. This is, to our knowledge, the largest cohort for this entity reported to date, with previous studies limited by lower patient numbers and/or usage of only targeted sequencing approaches.[40,52] In addition, the vast majority of lymphomas included in this study underwent rigorous pathology panel review and were molecularly classified by using the recently published Lymph3Cx assay.[13] Using MutSigCV, we describe a set of 50 putative driver genes with clear evidence of somatic mutation status in a considerable proportion of tumors. Given the relatively small sample size of our discovery cohort, we selected a *P* value cutoff of .05, representing a stringency level that balances biological discovery potential with the chance of false-positive findings. As expected from previous studies reporting single gene alterations, mutations affecting various members of the JAK-STAT and NF-κB pathways are highly enriched in PMBL, with *SOCS1* being the most frequently altered gene in our cohort. In concordance with the recent studies published by Dubois et al[40] and Mansouri et al,[52] we also found *ITPKB, MFHAS1* (malignant fibrous histiocytoma amplified sequence 1), *XPO1* (exportin 1), and *NFKBIE* to be frequently mutated in PMBL. A summary of the key findings of our study confirming and textualizing previous findings, as well as discovering novel disease biology, is presented in supplemental Figure 13.

Another prominent aspect of PMBL pathophysiology is the immune escape phenotype in this disease.[20] Consistent with this, we discovered recurrent genomic alterations in genes involved in MHC expression and MHC complex formation/stability (*B2M* and *CIITA*), interaction with NK cell subsets (*CD58*), and alteration of T cell–mediated immune response (*CD274* and *PDCD1LG2*), which have been, in part, extensively characterized before and were also recently reported in a series of 37 PMBL cases.[23,24,27,53] In addition to known recurrent aberrations, we

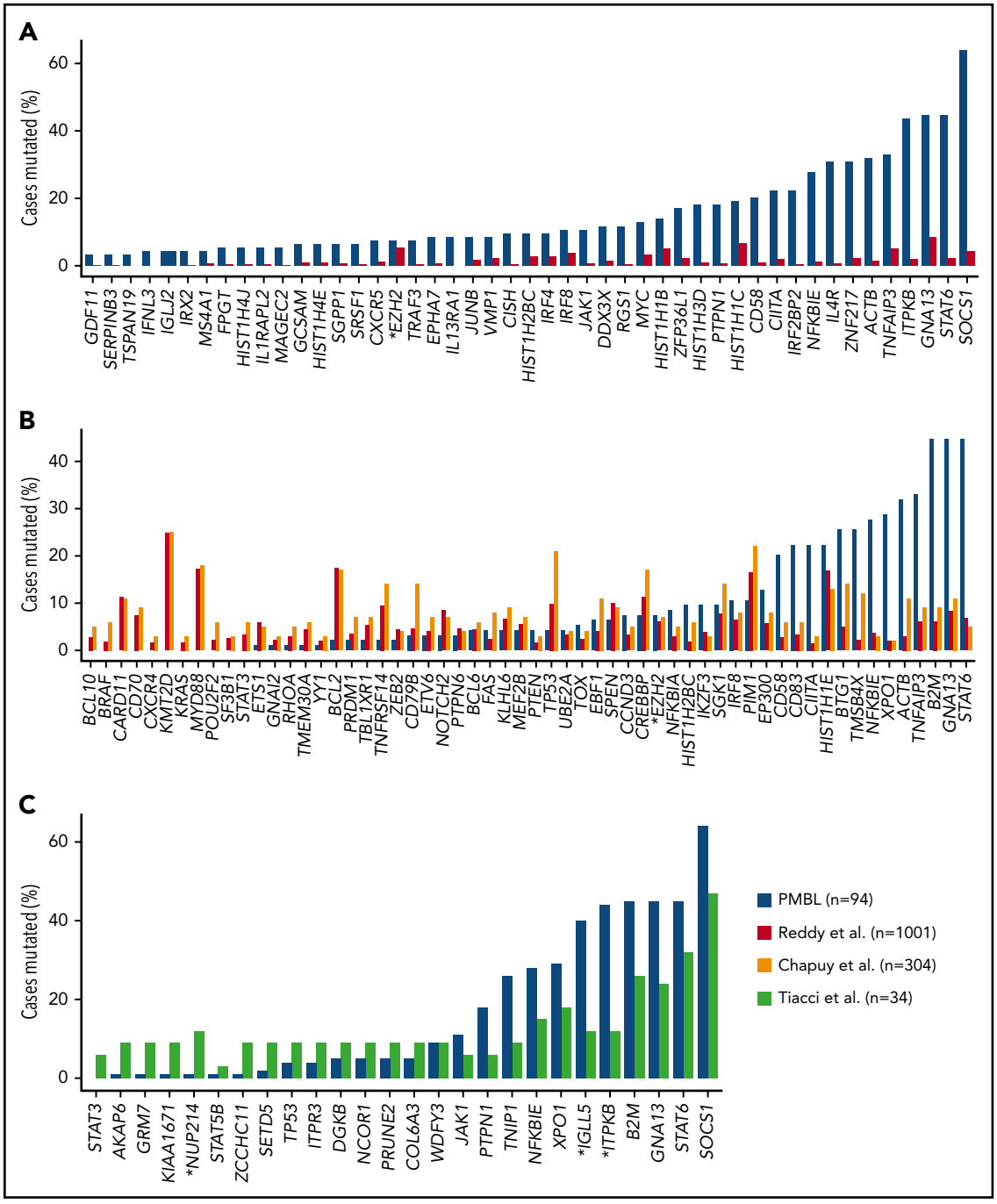

Figure 4. Comparison of mutational frequencies between histopathological/pathogenetically related entities. (A) Comparison of mutation frequencies for putative PMBL driver genes identified by MutSigCV between our PMBL cohort and the DLBCL cohort published by Reddy et al[48] (genes were required to be mutated in at least 3 cases). (B) Comparison of mutation frequencies in DLBCL driver genes as identified in Chapuy et al[4] between our PMBL cohort and the DLBCL cohorts published by Reddy et al and Chapuy et al; *EZH2* is marked by an asterisk in panels A and B, as the only gene with no significant difference in terms of mutational frequency between DLBCL and PMBL. (C) Mutational frequencies in cHL and PMBL are comparable for genes shown to be recurrently mutated in cHL as defined by Tiacci et al.[49] Statistically significant differences in mutation frequency between the two cohorts are marked with an asterisk. For all comparisons, silent as well as 5′- and 3′-UTR mutations were excluded.

have observed mutations in genes involved in interferon signaling in one half of the tumors (*IRF2BP2* in 22% of cases, *IRF8* in 12%, *IRF4* in 11%, and *CISH* in 10%). The transcription factors IRF4 and IRF8 are known to play an important role in B-cell/plasma cell development as well as in the germinal center response in a mutually antagonistic manner.[54,55] Interestingly, we found in 6 (54.5%) of 11 cases, a hotspot mutation *IRF4*: c.295T>C, p.(Cys99Arg) affecting the DNA-binding domain of IRF4. This specific nucleotide change has been previously observed in activated B-cell–like DLBCL,[40] although at lower relative frequencies compared with our study. To what extent this mutation constitutes IRF4-addiction in PMBL and a potential therapeutically targetable vulnerability needs to be determined in functional studies. Moreover, the interactions with other pathways known to play important roles in PMBL pathogenesis (eg, the JAK-STAT pathway) will need to be elucidated in the future.

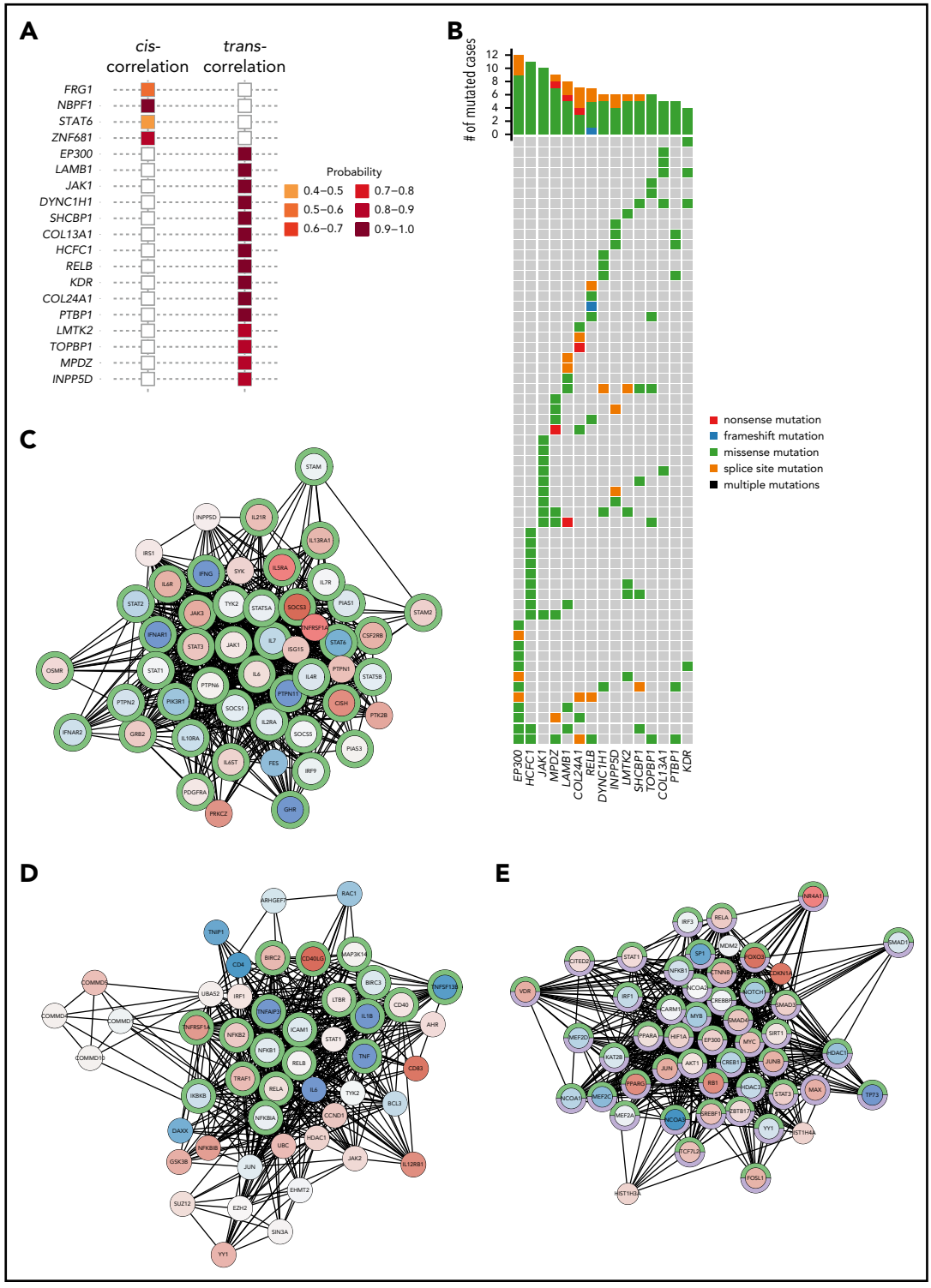

Figure 5. Impact of recurrent mutations on the transcriptome. (A) Plot displaying sets of genes identified as showing significant *cis*- or *trans*-effects on gene expression based on *xseq* analysis. (B) Oncoplot showing the distribution of mutations in genes with a *trans*-effect across the entire cohort. Gene association networks for significant *trans*-influencing genes exemplified by (C) *JAK1*, (D) *RELB*, and (E) *EP300* based on *xseq* analysis. Nodes represent genes within the interaction network, and edges are interactions between genes based on the global influence network (see "Methods" for details). Nodes are colored by average log2 normalized expression across patients whose tumors harbor mutations, with red indicating high expression and blue indicating low expression. Genes with green borders in the network are functionally enriched for the JAK-STAT signaling pathway (panel C, FDR, $P = 4.44E\text{-}72$) or the NF-κB signaling pathway (panel D, FDR, $P = 8.13E\text{-}27$), respectively. In panel E, the green and purple borders highlight genes enriched in pathways related to epigenetic regulation, specifically the regulation of transcription (FDR, $P = 8.3E\text{-}47$) and the regulation of nucleic acid–templated transcription (FDR, $P = 4.83E\text{-}43$), respectively.

By comparing mutational frequencies in PMBL and related pathological entities (DLBCL and cHL), we provide further evidence that PMBL is distinct from DLBCL not only on the gene expression level but also in terms of the mutational landscape and putative driver genes. Conversely, the majority of recurrently mutated genes in cHL are also frequently altered in PMBL, further establishing the pathophysiological relatedness of these 2 lymphoma entities.[8,9]

Our study also yielded specific genes (*JAK1*, *RELB*, and *EP300*) with disrupted expression triggered by genomic mutations in either the coding or the regulatory space. These results imply that mutated regulatory components of the genome contribute substantially to cancer pathways and show the importance of integrative analysis approaches to enhance biological interpretation of the PMBL mutational landscape and other cancers.

Recent publications in DLBCL[4,5] suggest that mutational profiles, either in isolation or in synergy with cell-of-origin–based classification (activated B-cell– vs germinal center B-cell–like DLBCL) and standard diagnostic tools such as fluorescence in situ hybridization or immunohistochemistry, can aid in more precise classification of aggressive B-cell lymphomas. Our finding of a distinct mutational landscape in PMBL, in contrast to DLBCL, and select mutations (eg, in *IL4R* and *TNFRSF14*) cosegregating with molecular signatures strongly suggest that mutational profiling should be evaluated to establish a new taxonomy for aggressive lymphomas and tested for clinical validity and utility alongside clinical trials and modern treatments of PMBL and related entities.

Acknowledgments

The authors are grateful to J. Ding for technical support implementing the *xseq* tool. The authors also thank the pathology panel members of the Lymphoma/Leukemia Molecular Profiling Project for central pathology review of all PMBL cases used in this study.

This work was supported by generous funding from the Terry Fox Research Institute through a Program Project grant (1023 and 1061, C. Steidl, J.C., and M.M.) and a Canadian Institutes of Health Research Foundation grant to C. Steidl. C. Steidl is supported by a Michael Smith Foundation for Health Research career investigator award and a Canadian Institutes of Health Research new investigator award. A. Mottok was supported by postdoctoral and research fellowships from the German Cancer Aid (Mildred-Scheel-Foundation), the Michael Smith Foundation for Health Research (MSFHR), and Lymphoma Canada, and currently receives funding through the Clinician Scientist Program at the Medical Faculty, University of Ulm. E.V. is supported by a Michael Smith Foundation for Health Research trainee award.

Authorship

Contribution: A. Mottok, S.S.H., E.A.C., and C. Steidl designed the study; A. Mottok, S.S.H., E.A.C., B.W., A.T., B.M., H.N., C.R., and S.B.-N. performed research; A. Mottok, S.S.H., L.C.C., C.R., E.V., C. Sarkozy, A. Mungall, M.A.M., R.S., and C. Steidl interpreted data; R.D.G., J.M.C., D.W.S., and K.J.S. provided clinical data and/or performed pathology review; A. Mottok, S.S.H., and C. Steidl wrote the manuscript; and all authors read and approved the final manuscript.

Conflict-of-interest disclosure: A. Mottok, D.W.S., and C. Steidl are named inventors on a patent filed by the National Cancer Institute "Methods for determining lymphoma type." K.J.S. has received honoraria from and consulted for Seattle Genetics, Bristol-Myers Squibb, Merck, Verastem, and AbbVie; has consulted for Servier; received honoraria from Takeda; and received institutional research funding from Roche. D.W.S. has served as a consultant for Janssen and Celgene; received research funding from Roche/Genentech, Janssen, and NanoString Technologies; received travel funding from Celgene; and is a named inventor on patents, including one licensed to NanoString Technologies (institution). C. Steidl has served as a consultant for Seattle Genetics, Roche, Bayer, and Curis; and has received research funding from Bristol-Myers Squibb and Tioma. The remaining authors declare no competing financial interests.

ORCID profiles: C.R., 0000-0001-6306-9361; S.B.-N., 0000-0002-2867-4037; A. Mungall, 0000-0002-0905-2742; M.A.M., 0000-0001-7146-7175; C. Steidl, 0000-0001-9842-9750.

Correspondence: Christian Steidl, Department of Lymphoid Cancer Research, British Columbia Cancer, 675 West 10th Ave, Vancouver, BC V5Z 1L3, Canada; e-mail: csteidl@bccancer.bc.ca.

Footnotes

Submitted 14 April 2019; accepted 28 June 2019. Prepublished online as *Blood* First Edition paper, 10 July 2019; DOI 10.1182/blood.2019001126.

*A.M. and S.S.H. contributed equally to this work.

The data reported in this article have been deposited in the Gene Expression Omnibus database (accession number GSE134511). Exomes are uploaded to the European Genome-Phenome Archive (accession number EGAS00001003746).

The online version of this article contains a data supplement.

There is a *Blood* Commentary on this article in this issue.

The publication costs of this article were defrayed in part by page charge payment. Therefore, and solely to indicate this fact, this article is hereby marked "advertisement" in accordance with 18 USC section 1734.

REFERENCES

1. Swerdlow S, Campo E, Harris N, Jaffe E. WHO Classification of Tumours of Haematopoietic and Lymphoid Tissues. Lyon, France: IARC Press; 2017.
2. Monti S, Chapuy B, Takeyama K, et al. Integrative analysis reveals an outcome-associated and targetable pattern of p53 and cell cycle deregulation in diffuse large B cell lymphoma. *Cancer Cell*. 2012;22(3):359-372.
3. Lenz G, Wright G, Dave SS, et al; Lymphoma/Leukemia Molecular Profiling Project. Stromal gene signatures in large-B-cell lymphomas. *N Engl J Med*. 2008;359(22):2313-2323.
4. Chapuy B, Stewart C, Dunford AJ, et al. Molecular subtypes of diffuse large B cell lymphoma are associated with distinct pathogenic mechanisms and outcomes [published correction appears in *Nat Med*. 2018;24(8):1292]. *Nat Med*. 2018;24(5):679-690.
5. Schmitz R, Wright GW, Huang DW, et al. Genetics and pathogenesis of diffuse large B-cell lymphoma. *N Engl J Med*. 2018;378(15):1396-1407.
6. Ennishi D, Jiang A, Boyle M, et al. Double-hit gene expression signature defines a distinct subgroup of germinal center B-cell-like diffuse large B-cell lymphoma. *J Clin Oncol*. 2019;37(3):190-201.
7. Alizadeh AA, Eisen MB, Davis RE, et al. Distinct types of diffuse large B-cell lymphoma identified by gene expression profiling. *Nature*. 2000;403(6769):503-511.
8. Rosenwald A, Wright G, Leroy K, et al. Molecular diagnosis of primary mediastinal B cell lymphoma identifies a clinically favorable subgroup of diffuse

large B cell lymphoma related to Hodgkin lymphoma. *J Exp Med*. 2003;198(6):851-862.

9. Savage KJ, Monti S, Kutok JL, et al. The molecular signature of mediastinal large B-cell lymphoma differs from that of other diffuse large B-cell lymphomas and shares features with classical Hodgkin lymphoma. *Blood*. 2003;102(12):3871-3879.

10. Möller P, Lämmler B, Eberlein-Gonska M, et al. Primary mediastinal clear cell lymphoma of B-cell type. *Virchows Arch A Pathol Anat Histopathol*. 1986;409(1):79-92.

11. Scott DW, Wright GW, Williams PM, et al. Determining cell-of-origin subtypes of diffuse large B-cell lymphoma using gene expression in formalin-fixed paraffin-embedded tissue. *Blood*. 2014;123(8):1214-1217.

12. Scott DW, Mottok A, Ennishi D, et al. Prognostic significance of diffuse large B-cell lymphoma cell of origin determined by digital gene expression in formalin-fixed paraffin-embedded tissue biopsies. *J Clin Oncol*. 2015;33(26):2848-2856.

13. Mottok A, Wright G, Rosenwald A, et al. Molecular classification of primary mediastinal large B-cell lymphoma using routinely available tissue specimens. *Blood*. 2018;132(22):2401-2405.

14. Yuan J, Wright G, Rosenwald A, et al; Lymphoma Leukemia Molecular Profiling Project (LLMPP). Identification of primary mediastinal large B-cell lymphoma at non-mediastinal sites by gene expression profiling. *Am J Surg Pathol*. 2015;39(10):1322-1330.

15. Sarkozy C, Copie-Bergman C, Damotte D, et al. Gray-zone lymphoma between cHL and large B-cell lymphoma: a histopathologic series from the LYSA. *Am J Surg Pathol*. 2019;43(3):341-351.

16. Traverse-Glehen A, Pittaluga S, Gaulard P, et al. Mediastinal gray zone lymphoma: the missing link between classic Hodgkin's lymphoma and mediastinal large B-cell lymphoma. *Am J Surg Pathol*. 2005;29(11):1411-1421.

17. Pilichowska M, Pittaluga S, Ferry JA, et al. Clinicopathologic consensus study of gray zone lymphoma with features intermediate between DLBCL and classical HL. *Blood Adv*. 2017;1(26):2600-2609.

18. Viganò E, Gunawardana J, Mottok A, et al. Somatic IL4R mutations in primary mediastinal large B-cell lymphoma lead to constitutive JAK-STAT signaling activation. *Blood*. 2018;131(18):2036-2046.

19. Lees C, Keane C, Gandhi MK, Gunawardana J. Biology and therapy of primary mediastinal B-cell lymphoma: current status and future directions. *Br J Haematol*. 2019;185(1):25-41.

20. Mottok A, Steidl C. Genomic alterations underlying immune privilege in malignant lymphomas. *Curr Opin Hematol*. 2015;22(4):343-354.

21. Ansell SM, Lesokhin AM, Borrello I, et al. PD-1 blockade with nivolumab in relapsed or refractory Hodgkin's lymphoma. *N Engl J Med*. 2015;372(4):311-319.

22. Zinzani PL, Ribrag V, Moskowitz CH, et al. Safety and tolerability of pembrolizumab in patients with relapsed/refractory primary mediastinal large B-cell lymphoma. *Blood*. 2017;130(3):267-270.

23. Steidl C, Shah SP, Woolcock BW, et al. MHC class II transactivator CIITA is a recurrent gene fusion partner in lymphoid cancers. *Nature*. 2011;471(7338):377-381.

24. Mottok A, Woolcock B, Chan FC, et al. Genomic alterations in CIITA are frequent in primary mediastinal large B cell lymphoma and are associated with diminished MHC class II expression. *Cell Reports*. 2015;13(7):1418-1431.

25. Green MR, Monti S, Rodig SJ, et al. Integrative analysis reveals selective 9p24.1 amplification, increased PD-1 ligand expression, and further induction via JAK2 in nodular sclerosing Hodgkin lymphoma and primary mediastinal large B-cell lymphoma. *Blood*. 2010;116(17):3268-3277.

26. Twa DDW, Chan FC, Ben-Neriah S, et al. Genomic rearrangements involving programmed death ligands are recurrent in primary mediastinal large B-cell lymphoma. *Blood*. 2014;123(13):2062-2065.

27. Chong LC, Twa DDW, Mottok A, et al. Comprehensive characterization of programmed death ligand structural rearrangements in B-cell non-Hodgkin lymphomas. *Blood*. 2016;128(9):1206-1213.

28. Bentz M, Barth TFE, Brüderlein S, et al. Gain of chromosome arm 9p is characteristic of primary mediastinal B-cell lymphoma (MBL): comprehensive molecular cytogenetic analysis and presentation of a novel MBL cell line. *Genes Chromosomes Cancer*. 2001;30(4):393-401.

29. Li H, Durbin R. Fast and accurate long-read alignment with Burrows-Wheeler transform. *Bioinformatics*. 2010;26(5):589-595.

30. Koboldt DC, Chen K, Wylie T, et al. VarScan: variant detection in massively parallel sequencing of individual and pooled samples. *Bioinformatics*. 2009;25(17):2283-2285.

31. Saunders CT, Wong WS, Swamy S, Becq J, Murray LJ, Cheetham RK. Strelka: accurate somatic small-variant calling from sequenced tumor-normal sample pairs. *Bioinformatics*. 2012;28(14):1811-1817.

32. Cibulskis K, Lawrence MS, Carter SL, et al. Sensitive detection of somatic point mutations in impure and heterogeneous cancer samples. *Nat Biotechnol*. 2013;31(3):213-219.

33. Hiltemann S, Jenster G, Trapman J, van der Spek P, Stubbs A. Discriminating somatic and germline mutations in tumor DNA samples without matching normals. *Genome Res*. 2015;25(9):1382-1390.

34. Sherry ST, Ward MH, Kholodov M, et al. dbSNP: the NCBI database of genetic variation. *Nucleic Acids Res*. 2001;29(1):308-311.

35. Cingolani P, Platts A, Wang L, et al. A program for annotating and predicting the effects of single nucleotide polymorphisms, SnpEff: SNPs in the genome of Drosophila melanogaster strain w1118; iso-2; iso-3. *Fly (Austin)*. 2012;6(2):80-92.

36. Lawrence MS, Stojanov P, Polak P, et al. Mutational heterogeneity in cancer and the search for new cancer-associated genes. *Nature*. 2013;499(7457):214-218.

37. Talevich E, Shain AH, Botton T, Bastian BC. CNVkit: genome-wide copy number detection and visualization from targeted DNA sequencing. *PLOS Comput Biol*. 2016;12(4):e1004873.

38. Beroukhim R, Getz G, Nghiemphu L, et al. Assessing the significance of chromosomal aberrations in cancer: methodology and application to glioma. *Proc Natl Acad Sci U S A*. 2007;104(50):20007-20012.

39. Ding J, McConechy MK, Horlings HM, et al. Systematic analysis of somatic mutations impacting gene expression in 12 tumour types. *Nat Commun*. 2015;6(1):8554.

40. Dubois S, Viailly PJ, Mareschal S, et al. Next-generation sequencing in diffuse large B-cell lymphoma highlights molecular divergence and therapeutic opportunities: a LYSA study. *Clin Cancer Res*. 2016;22(12):2919-2928.

41. Gunawardana J, Chan FC, Telenius A, et al. Recurrent somatic mutations of PTPN1 in primary mediastinal B cell lymphoma and Hodgkin lymphoma. *Nat Genet*. 2014;46(4):329-335.

42. Melzner I, Weniger MA, Bucur AJ, et al. Biallelic deletion within 16p13.13 including SOCS-1 in Karpas1106P mediastinal B-cell lymphoma line is associated with delayed degradation of JAK2 protein. *Int J Cancer*. 2006;118(8):1941-1944.

43. Ritz O, Guiter C, Castellano F, et al. Recurrent mutations of the STAT6 DNA binding domain in primary mediastinal B-cell lymphoma. *Blood*. 2009;114(6):1236-1242.

44. Tamborero D, Gonzalez-Perez A, Lopez-Bigas N. OncodriveCLUST: exploiting the positional clustering of somatic mutations to identify cancer genes. *Bioinformatics*. 2013;29(18):2238-2244.

45. Alexandrov LB, Nik-Zainal S, Wedge DC, et al; ICGC PedBrain. Signatures of mutational processes in human cancer [published correction appears in *Nature*. 2013;502(7470):258.]. *Nature*. 2013;500(7463):415-421.

46. Gröbner SN, Worst BC, Weischenfeldt J, et al; ICGC MMML-Seq Project. The landscape of genomic alterations across childhood cancers [published correction appears in *Nature*. 2018;559(7714):E10]. *Nature*. 2018;555(7696):321-327.

47. Wessendorf S, Barth TF, Viardot A, et al. Further delineation of chromosomal consensus regions in primary mediastinal B-cell lymphomas: an analysis of 37 tumor samples using high-resolution genomic profiling (array-CGH). *Leukemia*. 2007;21(12):2463-2469.

48. Reddy A, Zhang J, Davis NS, et al. Genetic and functional drivers of diffuse large B cell lymphoma. *Cell*. 2017;171(2):481-494.e15.

49. Tiacci E, Ladewig E, Schiavoni G, et al. Pervasive mutations of JAK-STAT pathway genes in classical Hodgkin lymphoma. *Blood*. 2018;131(22):2454-2465.

50. Kasper LH, Boussouar F, Ney PA, et al. A transcription-factor-binding surface of coactivator p300 is required for haematopoiesis. *Nature*. 2002;419(6908):738-743.

51. Morin RD, Mendez-Lago M, Mungall AJ, et al. Frequent mutation of histone-modifying genes in non-Hodgkin lymphoma. *Nature*. 2011;476(7360):298-303.

52. Mansouri L, Noerenberg D, Young E, et al. Frequent NFKBIE deletions are associated with poor outcome in primary mediastinal B-cell lymphoma. *Blood*. 2016;128(23):2666-2670.

53. Chapuy B, Stewart C, Dunford A, et al. Comprehensive genomic analysis of primary mediastinal B-cell lymphoma. *Blood*. 2018;132(suppl 1):1564.

54. Xu H, Chaudhri VK, Wu Z, et al. Regulation of bifurcating B cell trajectories by mutual antagonism between transcription factors IRF4 and IRF8. *Nat Immunol*. 2015;16(12):1274-1281.

55. Ochiai K, Maienschein-Cline M, Simonetti G, et al. Transcriptional regulation of germinal center B and plasma cell fates by dynamical control of IRF4. *Immunity*. 2013;38(5):918-929.